KSME Journal, Vol. 2, No. 1, pp. 63~68, 1988.

OUTPUT FEEDBACK CONTROL OF ROTATING DISK VIBRATIONS

Chul-Soo Kim* and Chong-Won Lee*

(Received April 11, 1988)

Output feedback control of rotating disk vibrations is investigated. A polynomial equation, which determines the closed-loop system poles, is derived in wave coordinates and the approximate solutions for each wave are provided. The closed-loop system characteristics are analyzed in relation to the P-D gains and the sensor-actuator location, utilizing the approximate solutions of the closed-loop poles. Analysis of the closed-loop system in case of the half-clamped disk is also performed, with the gains and location varied.

Key Words: Output Feedback Control, Rotating Disk Vibrations, Travelling Wave, Wave Coordinates, Modal State, P-D gains

1. INTRODUCTION

Vibration control of rotating disks has attracted the attention of many investigators in recent years especially in the fields of circular saws and computer memory disks in an attempt to reduce the vibration during operation(Ellis and Mote, 1979, Radcliffe and Mote, 1983, Iwan and Moeller, 1976, Cho and Cho, 1981, Kim and Lee 1988, Byun and Lee 1988). In 1979, Ellis and Mote first performed active control to reduce the circular disk vibration, in which proportional and derivative control was implemented employing a pair of electromagnetic actuators and a displacement sensor. Their works, however, were limited to some experimental results without deep comprehension of the closed-loop system characteristics, although the roles of proportional and derivative control gains in rotating disks differ from those in stationary disks.

Unlike nonrotating flexible systems, modal distributions of a rotating disk are characterized by pairs of waves propagating in the opposite directions along the periphery of the disk. The waves propagating in the direction and in the opposite direction of disk rotation are called forward and backward travelling waves, respectively. The frequencies of both travelling waves seen by a stationary observer change as the disk rotation speed increases, the frequency of the forward travelling wave being increased and that of the backward travelling wave being decreased(Mote, 1970). As reported in the literature(Mote and Holoyen, 1975), the backward travelling waves of low frequencies are important to the disk vibration. Hence, vibration control of rotating disk often aims at suppressing the lower backward travelling waves. However, as a result, the control efforts concentrate in forward travelling waves of high frequencies, which may result in instability of the closed-loop system in case that the phase-shift at high frequency exists.

*Department of Mechanical Engineering, Korea Advanced Institute of Science and Technology Seoul 130-650, Korea.

In this paper, we will investigate the stability of the rotating disk under P-D control action and the roles of control gains about each travelling wave with the aid of the approximate solutions. In addition, the analysis of the roles of each control gain associated with the sensor location is included. To obtain the approximate solutions, it requires the state space formulation represented in wave coordinates, which is derived by our previous works(Kim and Lee 1988), rather than the conventional state space formulation in which both travelling waves are inherently coupled. It is summarized in the next section.

2. EQUATION OF MOTION IN MODAL STATE SPACE

Consider a uniform, annular disk with clamped inner radius $R=a$ and free outer radius $R=b$ as shown in Fig. 1. If the transverse displacement $W(R, \theta, t)$ of the disk is small and the disk is slightly damped, then the equation of motion of the disk subject to $Q(R, \theta, t)$, the transverse excitation force per unit area, is given in a non-dimensionalized form as(Byun and Lee 1988)

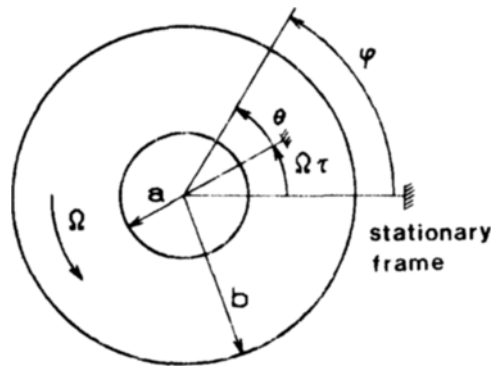

Fig. 1 Configuration of a centrally clamped disk

$$w_{,\tau\tau}+2\alpha w_{,\tau}+A_0 w=q(r,\theta,\tau) \tag{1}$$

where

$$A_0=\frac{E}{3\rho(1-\nu^2)}\frac{h^2}{b^4\mu_{10}^2}\nabla^4$$

Here nondimensional parameters are the displacement $w=W/b$, the radius $r=R/b$, the time $\tau=\mu_{10}t$ and the transverse excitation $q=Q/2\rho hb\mu_{10}^2$. And ρ is the density of the disk, E the elastic modulus, h the half-thickness, ν Poisson's ratio, α the damping coefficient of the disk, μ_{10} the natural frequency of the non-rotating disk corresponding to the vibration mode with one nodal diameter and zero nodal circle, and R and θ are the polar coordinates of a point on the disk.

As the disk rotates at the rotational speed Ω_{rot}, the external force may be treated as a moving load with the angular velocity of $-\Omega_{rot}$ with respect to the rotating(body fixed) coordinates. The moving load problem(Eq. 1) can be transformed into the rotating disk problem subjected to the stationary load(Iwan and Moeller, 1976), using the relationships between the rotating(body fixed) coordinates(r,θ) and the stationary(inertial) coordinates(r,φ),

$$\begin{aligned}&\varphi=\theta+\Omega\tau\\ &w_{,\tau}=v_{,\tau}+\Omega v_{,\varphi}\\ &w_{,\tau\tau}=v_{,\tau\tau}+2\Omega v_{,\tau\varphi}+\Omega^2 v_{,\varphi\varphi}\end{aligned} \tag{2}$$

where v is the dimensionless transverse displacement, φ the angular position in the inertial coordinates and $\Omega=\Omega_{rot}/\mu_{10}$ the nondimensional rotational speed. Substituting Eq. (2) into Eq. (1), the equation of motion is rewritten as

$$\begin{aligned}&v_{,\tau\tau}+2\Omega v_{,\tau\varphi}+\Omega^2 v_{,\varphi\varphi}+A_0 v+2\alpha(v_{,\tau}+\Omega v_{,\varphi})\\ &=f(r,\varphi,\tau)\end{aligned} \tag{3}$$

where f is the dimensionless control force in the inertial coordinates(r,φ).

Eq. (3) can be written in state space as, when $f=0$,

$$\dot{x}_v(\tau)=A_v x_v(\tau) \tag{4}$$

where $x_v(\tau)=\begin{Bmatrix}v(\cdot,\cdot,\tau)\\ v_{,\tau}(\cdot,\cdot,\tau)\end{Bmatrix}$

and $A_v=\begin{bmatrix}0 & 1\\ -A_0-\Omega^2\dfrac{\partial^2}{\partial\varphi^2}-2\alpha\Omega\dfrac{\partial}{\partial\varphi} & -2\Omega\dfrac{\partial}{\partial\varphi}-2\alpha\end{bmatrix}$

The response of Eq. (4) can be represented by the complex series expansion(Kim and Lee, 1988)

$$x_v=\sum_{m,n=0}^{\infty}[C_{mn}^b\phi_{mn}^b+C_{mn}^f\phi_{mn}^f+\bar{C}_{mn}^b\bar{\phi}_{mn}^b+\bar{C}_{mn}^f\bar{\phi}_{mn}^f] \tag{5}$$

where

$$\phi_{mn}^b=\begin{Bmatrix}V_{mn}\\ \lambda_{mn}^b V_{mn}\end{Bmatrix},\quad \phi_{mn}^f=\begin{Bmatrix}V_{mn}\\ \lambda_{mn}^f V_{mn}\end{Bmatrix}$$

and $\lambda_{mn}^b=-\alpha+j(m\Omega-\omega_{mnd}),\quad \lambda_{mn}^f=-\alpha+j(m\Omega+\omega_{mnd})$

$$\omega_{mnd}^2=\omega_{mn}^2+\alpha^2$$

$$V_{mn}(r,\varphi)=\frac{1}{2}e^{-jm\varphi}R_{mn}(r)$$

Here, λ_{mn}^i and ϕ_{mn}^i, $i=b,f$, are the eigenvalues and the corresponding eigenvectors of A_v, respectively, and m,n denote the number of nodal diameters and nodal circles, respectively, and the superscripts b and f denote the backward and forward travelling waves, respectively, ω_{mn} is the natural frequency of (m,n) mode in body-fixed coordinates, and $R_{mn}(r)$ is the radial mode shape function, which is normalized as

$$\int_{a/b}^{1} rR_{mn}(r)R_{ln}(r)\,dr=\frac{1}{\pi}\delta_{lm} \tag{6}$$

The adjoint, A_v^*, of A_v is found to be

$$A_v^*=\begin{bmatrix}0 & -1\\ A_0+\Omega^2\dfrac{\partial^2}{\partial\varphi^2}-2\alpha\Omega\dfrac{\partial}{\partial\varphi} & 2\Omega\dfrac{\partial}{\partial\varphi}-2\alpha\end{bmatrix}$$

with respect to the energy inner product

$$\left\langle\begin{Bmatrix}v\\ v_{,\tau}\end{Bmatrix},\begin{Bmatrix}v\\ v_{,\tau}\end{Bmatrix}\right\rangle_E=\langle A_0 v,v\rangle+\langle v_{,\tau}+\Omega v_{,\varphi},v_{,\tau}+\Omega v_{,\varphi}\rangle \tag{7}$$

where the inner product is defined as

$$\langle U,V\rangle=\int_{a/b}^{1}\int_0^{2\pi}V^T U r\,d\varphi\,dr \tag{8}$$

The two terms in the right hand side of Eq. (7) then correspond to the potential and kinetic energy. The eigenvectors associated with A_v^* are obtained to be

$$\left.\begin{aligned}\psi_{mn}^b&=K\begin{Bmatrix}V_{mn}\\ -\bar{\lambda}_{mn}^b V_{mn}\end{Bmatrix},\quad \bar{\psi}_{mn}^b\\ \psi_{mn}^f&=\bar{K}\begin{Bmatrix}V_{mn}\\ -\bar{\lambda}_{mn}^f V_{mn}\end{Bmatrix},\quad \bar{\psi}_{mn}^f\end{aligned}\right\}$$

where $1/K=\omega_{mnd}^2+j\alpha\omega_{mnd}$. The obtained eigenvectors of A_v and A_v^* may be biorthonormalized such that

$$\begin{aligned}&\langle A_v\phi_{mn}^i,\psi_{pq}^j\rangle_E=\lambda_{mn}^i\delta_{mp}\delta_{nq}\delta_{ij}\\ &\langle\phi_{mn}^i,\psi_{pq}^j\rangle_E=\delta_{mp}\delta_{nq}\delta_{ij},\quad i,j=b,f\end{aligned} \tag{9}$$

3. CONTROL SYSTEM AND CLOSED-LOOP POLES

In a case when the control system has one pointwise actuator located at the point(r_a,φ_a) and one pointwise displacement and one pointwise velocity sensors located at the same point(r_s,φ_s), the control force f and the measured output vector y may be expressed, respectively, as

$$f(r,\varphi,\tau)=F(\tau)\delta\left(\frac{r-r_a}{r_a}\right)\delta(\varphi-\varphi_a) \tag{10}$$

and

$$y(\tau)=\begin{Bmatrix}v(r_s,\varphi_s,\tau)\\ \dot{v}(r_s,\varphi_s,\tau)\end{Bmatrix} \tag{11}$$

Here, we may assume $\varphi_a=0$, without loss of generality, because only the relative position angle between the actuator and the sensors is meaningful. If we further assume that $r_a=$

$r_s = r_0$, then the open-loop system is represented in state space as,

$$\dot{x}_v(\tau) = A_v x_v(\tau) + Bu(\tau) \tag{12}$$

$$y(\tau) = (\langle x_v, \begin{Bmatrix} d \\ 0 \end{Bmatrix}\rangle, \langle x_v, \begin{Bmatrix} 0 \\ d \end{Bmatrix}\rangle)^T \tag{13}$$

where,

$$B = (0, \delta\left(\frac{r-r_0}{r_0}\right)\delta(\varphi))^T$$
$$d = \delta\left(\frac{r-r_0}{r_0}\right)\delta(\varphi-\varphi_s)$$
$$u(\tau) = F(\tau)$$

Also, the conventional P-D control law with negative output feedback can be written as

$$u(\tau) = -(k_p \quad k_d) y(\tau) \tag{14}$$

where the positive constants k_p, k_d are the proportional and derivative feedback gains, respectively. Combining Eqs. (12), (13) and (14), we obtain the closed-loop equation.

$$\dot{x}_v = (A_v + B\langle \cdot, G\rangle) x_v \tag{15}$$

where $G = -(k_p d \quad k_d d)$. From the results of degenerate perturbations (Kato, 1966), we see that the closed-loop poles are determined by the zeros of the polynomial

$$h(\lambda) = 1 + \langle (A_v - \lambda)^{-1} B, G\rangle \tag{16}$$

Here, we note that the resolvent $R(\lambda, A_v)$ becomes

$$\begin{aligned} R(\lambda, A_v) &= (\lambda - A_v)^{-1} \\ &= \sum_{m,n=0}^{\infty}\Big[\frac{1}{\lambda-\lambda_{mn}^b}\langle \cdot, \psi_{mn}^b\rangle_E \phi_{mn}^b \\ &+ \frac{1}{\lambda-\bar{\lambda}_{mn}^b}\langle \cdot, \bar{\psi}_{mn}^b\rangle_E \bar{\phi}_{mn}^b \\ &+ \frac{1}{\lambda-\lambda_{mn}^f}\langle \cdot, \psi_{mn}^f\rangle_E \phi_{mn}^f \\ &+ \frac{1}{\lambda-\bar{\lambda}_{mn}^f}\langle \cdot, \bar{\psi}_{mn}^f\rangle_E \bar{\phi}_{mn}^f\Big] \end{aligned} \tag{17}$$

Thus, Eq. (16) becomes

$$\begin{aligned} h(\lambda) &= 1 + \sum_{m,n=0}^{\infty}\Big[\frac{1}{\lambda-\lambda_{mn}^b}\langle B, \psi_{mn}^b\rangle_E\langle \phi_{mn}^b, G\rangle \\ &+ \frac{1}{\lambda-\bar{\lambda}_{mn}^b}\langle B, \bar{\psi}_{mn}^b\rangle_E\langle \bar{\phi}_{mn}^b, G\rangle \\ &+ \frac{1}{\lambda-\lambda_{mn}^f}\langle B, \psi_{mn}^f\rangle_E\langle \phi_{mn}^f, G\rangle \\ &+ \frac{1}{\lambda-\bar{\lambda}_{mn}^f}\langle B, \bar{\psi}_{mn}^f\rangle_E\langle \bar{\phi}_{mn}^f, G\rangle\Big] \\ &= 1 + \sum_{m,n=0}^{\infty}\frac{R_{mn}^2(r_0)}{4\omega_{mn}}\Big[\frac{je^{-jm\varphi_s}}{\lambda-\lambda_{mn}^b}(k_p + k_d\lambda_{mn}^b) \\ &+ \frac{-je^{jm\varphi_s}}{\lambda-\bar{\lambda}_{mn}^b}(k_p + k_d\bar{\lambda}_{mn}^b) + \frac{-je^{-jm\varphi_s}}{\lambda-\lambda_{mn}^f}(k_p + k_d\lambda_{mn}^f) \\ &+ \frac{je^{jm\varphi_s}}{\lambda-\bar{\lambda}_{mn}^f}(k_p + k_d\bar{\lambda}_{mn}^f)\Big] \end{aligned} \tag{18}$$

In order to fully understand the nature of the closed-loop system, we should solve for the zeros of this polynomial equation, which is almost impossible. In order to obtain approximate solutions, a reduced order model, consisting of N modes(N pairs of backward and forward travelling waves) with zero nodal circle dominating the vibration, is treated in this work. In practice, the rotating disk vibration is not likely to be dominated by the modes with nodal circles in case of the centrally-clamped disk. For example, the saw transverse vibration is most often dominated by 0-6 nodal diameter modes with zero nodal circle. The modes with one or more nodal circles are unlikely to be excited in the cutting process. Thus Eq. (18) can be reduced to

$$\begin{aligned} h_N(\lambda) &= 1 + \sum_{m=0}^{N}\frac{R_m^2(r_0)}{4\omega_{md}}\Big[\frac{je^{-jm\varphi_s}}{\lambda-\lambda_m^b}(k_p + k_d\lambda_m^b) \\ &+ \frac{-je^{jm\varphi_s}}{\lambda-\bar{\lambda}_m^b}(k_p + k_d\bar{\lambda}_m^b) + \frac{-je^{-jm\varphi_s}}{\lambda-\lambda_m^f}(k_p + k_d\lambda_m^f) \\ &+ \frac{je^{jm\varphi_s}}{\lambda-\bar{\lambda}_m^f}(k_p + k_d\bar{\lambda}_m^f)\Big] \end{aligned} \tag{19}$$

Here and henceforth, the subscript $n=0$ is omitted for notational simplicity.

Although the exact solutions of Eq. (19) can be numerically calculated, it is worth obtaining the approximite solutions of Eq. (19) in order to look into the pole shifting behaviors due to control. Assuming the modeled waves are not severely overlapped and the eigenvalue perturbations due to control are fairly small, the approximate eigenvalues σ_m^b and σ_m^f, corresponding to the unperturbed eigenvalues λ_m^b and λ_m^f of $(m, 0)$ mode, respectively, are determined from

$$\sigma_m^b = \lambda_m^b - je^{-jm\varphi_s}P_m(k_p + k_d\lambda_m^b) \tag{20}$$

and

$$\sigma_m^f = \lambda_m^f + je^{-jm\varphi_s}P_m(k_p + k_d\lambda_m^f) \tag{21}$$

where

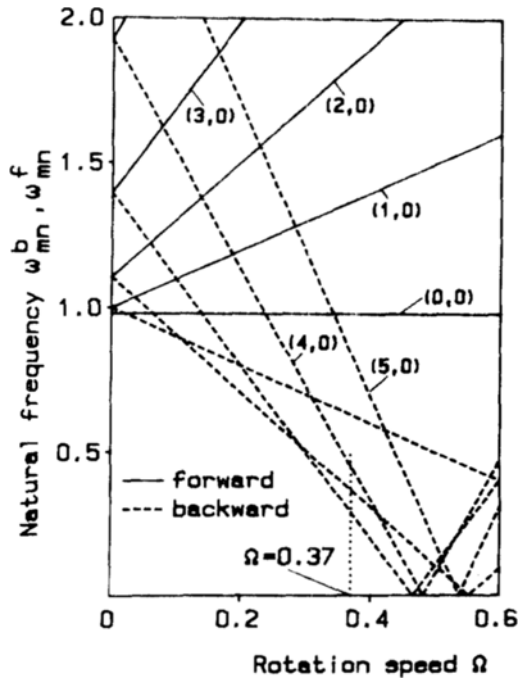

Fig. 2 The behavior of the observed natural frequencies w.r.t.Ω

$$P_m=\frac{R_m^2(r_0)}{4\omega_{md}}$$

The first order approximate bound of the approximate eigenvalues becomes(Kim and Lee, 1988)

$$|\gamma_m^i-\sigma_m^i|<|h_N(\sigma_m^i)/h_N'(\sigma_m^i)|,\quad i=b,f$$

where γ_m^i's are the eigenvalues of the closed-loop system, Eq. (19), and $h_N'(\cdot)$ is the derivative of $h_N(\cdot)$.

Now, we will investigate the effects of P-D gains and sensor location on the stability of the half-clamped disk with $r_0=1$, $\alpha=0.005$ and $N=6$, based upon the above approximate solutions. The methodology, which will be demonstrated in the next section, can be easily extended to the general centrally-clamped disk problems. The rotating disk with the clamping ratio of 0.5(=a/b) has the lowest critical speed of about 0.466, at which the frequency of backward travelling wave of (3,0) mode becomes zero as shown in Fig. 2.

4. ROLES OF P-D GAINS AND SENSOR LOCATION

To avoid too much complexity in analysis, P and D controls will be considered separately. In case of P-control($k_p\neq 0$, $k_d=0$), the approximate eigenvalues of the closed-loop system, Eqs. (20) and (21), become

$$\sigma_m^b=\lambda_m^b-je^{-jm\varphi_s}P_mk_p \tag{22}$$

and

$$\sigma_m^f=\lambda_m^f+je^{-jm\varphi_s}P_mk_p \tag{23}$$

When $\varphi_s=0$, i.e., the actuator and sensor locations are identical, Eqs. (22) and (23) become

$$\sigma_m^b=\lambda_m^b-jP_mk_p=-\alpha+j(m\Omega-\omega_{md}') \tag{24}$$
$$\sigma_m^f=\lambda_m^f+jP_mk_p=-\alpha+j(m\Omega+\omega_{md}') \tag{25}$$

where $\omega_{md}'=\omega_{md}+P_mk_p$, which can be interpreted as the controlled natural frequency of $(m, 0)$ mode of the disk in the body fixed coordinates. That is, the natural frequency of $(m, 0)$ mode in body fixed coordinates and, therefore, the critical speed increases as k_p increases. Fig. 3 shows the variation of the natural frequencies of both travelling waves of (3, 0) mode in the inertial coordinates as Ω increases when k_p is fixed as 0.2 and the other modes are not included to avoid the complexity in the calculation of eigenvalues due to the mode coupling. As shown in Fig. 3, the natural frequencies of both travelling waves increase below the critical speed, but the natural frequency of the backward travelling wave decreases beyond a rotating speed slightly over the critical speed. In addition, we note that, as $\omega_{md}\to\infty$, $P_mk_p\to 0$ and $\omega_{md}'\to\omega_{md}$ for fixed k_p, i.e., the higher modes in stationary disks are unaffected by the proportional control.

Next, we consider the case when $\varphi_s\neq 0$ to find the role of P-gain associated with sensor location. Eqs. (22) and (23) can be rewritten as

$$\sigma_m^b=-\alpha-P_mk_p\sin m\varphi_s-j(\omega_{md}-m\Omega+P_mk_p\cos m\varphi_s) \tag{26}$$
$$\sigma_m^f=-\alpha+P_mk_p\sin m\varphi_s+j(\omega_{md}+m\Omega+P_mk_p\cos m\varphi_s) \tag{27}$$

Here, notice that the second terms in above equations possess

Table 1 Nondimensionalized natural frequencies of the half-clamped disk at the rotation speed $\Omega=0.37$

(m,n) Mode	Backward	Forward
(1, 0)	0.63	1.37
(2, 0)	0.3664	1,8464
(3, 0)	0.2867	2.5067

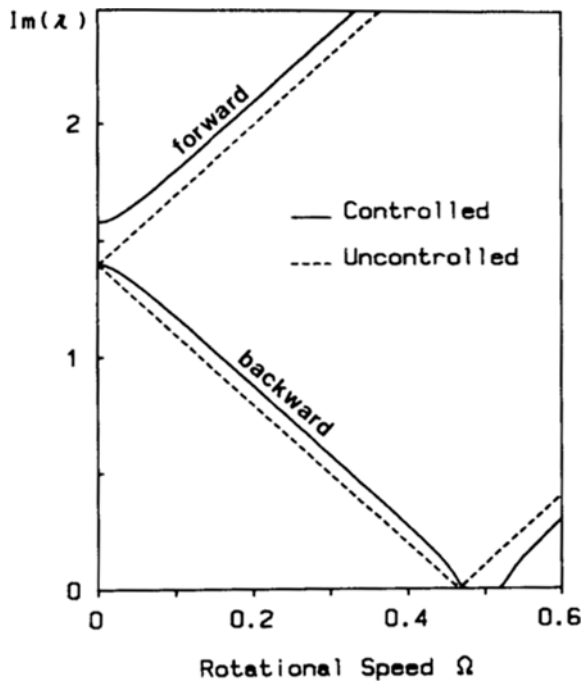

Fig. 3 Loci of natural frequencies of (3, 0) mode w.r.t.Ω for the case when (3, 0) mode is only considered; $k_p=0.2$

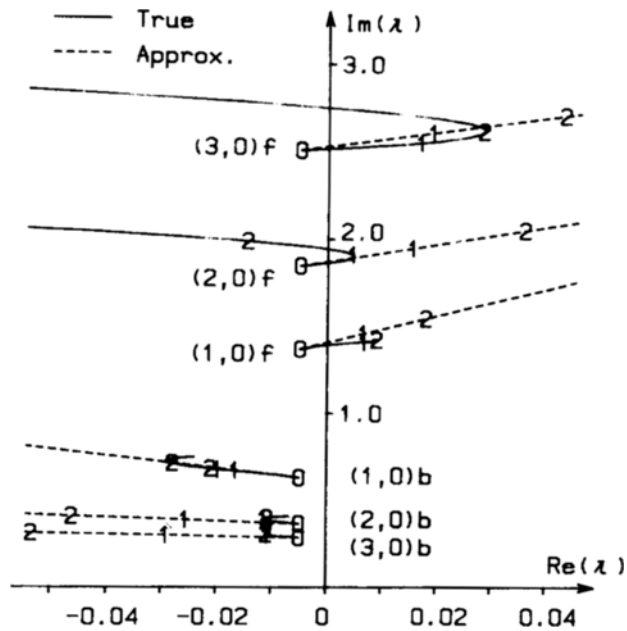

Fig. 4 Root loci of (1, 0), (2, 0) and (3, 0) modes as k_p increases when $\varphi_s=10$ degrees (1 ; $k_p=0.1$, 2 ; $k_p=0.2$)

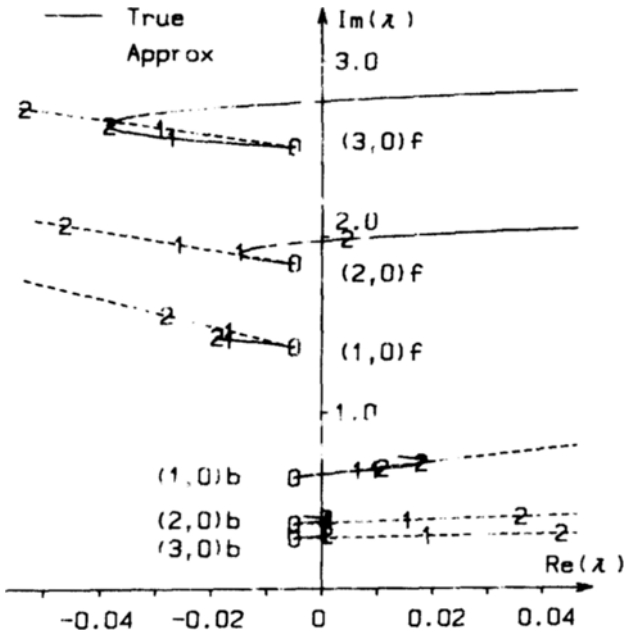

Fig. 5 Root loci of (1, 0), (2, 0) and (3, 0) modes as k_p increases when $\varphi_s = -10$ degrees (1 ; $k_p = 0.1$, 2 ; $k_p = 0.2$)

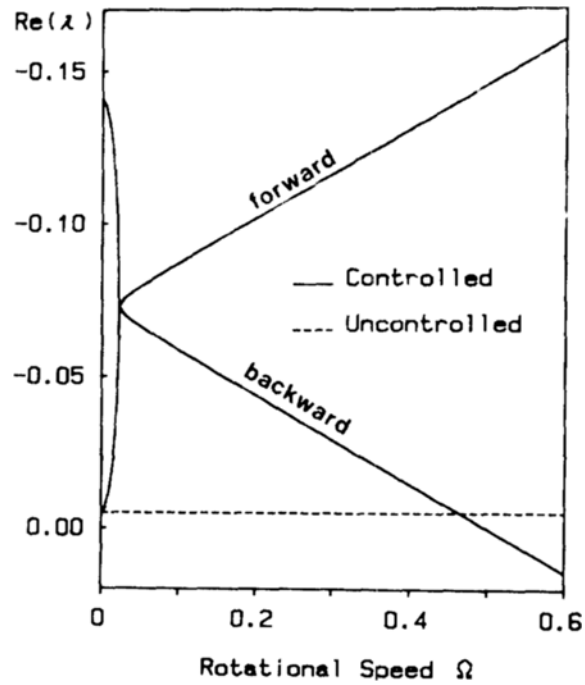

Fig. 6 Real part loci of the eigenvalues of (3, 0) mode w.r.t.Ω for the case when (3, 0) mode is only considered and $k_d = 0.1$

the opposite sign, which are closely related to the damping on the stability of travelling waves. For example, the damping of backward travelling waves increases, but that of forward travelling waves decreases for the modes satisfying $0 < m\varphi_s < \pi$. For the nondimensional rotation speed $\Omega = 0.37$(about 80% of the critical speed), the nondimensionalized natural frequencies of the travelling waves with 1 to 3 nodal diameters and zero nodal circle are tabulated in Table 1. Figs. 4 and 5 show the loci of the closed-loop eigenvalues of the modes with 1 to 3 nodal diameters and zero nodal circle as the proportional gain k_p increases when the derivative gain k_d is zero and the sensor location φ_s is equal to 10 and -10 degrees, respectively. The solid lines are the loci of the closed-loop eigenvalues calculated from Eq. (19) when $N = 6$, and the dashed lines are the loci of the closed-loop eigenvalues obtained from the approximate solutions, Eqs. (26) and (27). As shown in Figs. 4 and 5, the true solutions have the same trends as the approximate solutions up to $k_p = 0.1$. In this range of k_p, the forward waves may become unstable for the sensor location $\varphi_s = 10$ and the backward waves tend to become unstable for $\varphi_s = -10$ as the proportional gain k_p initially increases.

Now we consider the case of D-control($k_d \neq 0$, $k_p = 0$). In this case, the approximate eigenvalues of the closed-loop system, Eqs. (20) and (21), become

$$\sigma_m^b = \lambda_m^b - jP_m k_d \lambda_m^b \, e^{-jm\varphi_s} \tag{28}$$

and

$$\sigma_m^f = \lambda_m^f + jP_m k_d \lambda_m^f e^{-jm\varphi_s} \tag{29}$$

When $\varphi_s = 0$, Eqs. (28) and (29) become

$$\begin{aligned}\sigma_m^b &= \lambda_m^b - jP_m k_d \lambda_m^b \\ &= -\alpha - P_m k_d(\omega_{md} - m\Omega) - j(\omega_{md} - m\Omega - \alpha P_m k_d)\end{aligned} \tag{30}$$

$$\begin{aligned}\sigma_m^f &= \lambda_m^f + jP_m k_d \lambda_m^f \\ &= -\alpha - P_m k_d(\omega_{md} + m\Omega) + j(\omega_{md} + m\Omega - \alpha P_m k_d)\end{aligned} \tag{31}$$

Here, we can see that, for fixed k_d, $P_m k_d(\omega_{md} - m\Omega)$ in Eq. (30) decreases, but $P_m k_d(\omega_{md} + m\Omega)$ in Eq. (31) increases as the rotation speed of the disk increases up to the critical speed. In other words, the dampings (negative real parts of the eigenvalues) of the controlled forward (backward) waves are increased(decreased) as the rotation speed of the disk increases, in the derivative control of rotating disks, implying that the control efforts are put on the forward travelling waves not dominant in the disk vibration. Fig. 6 shows the real part of loci of the closed-loop eigenvalues of (3, 0) mode as Ω increases when k_d is 0.1 and the other modes are not included in calculation of the closed-loop eigenvalues as the same as in Fig. 3. As shown in Fig. 6, the damping of the forward travelling wave of (3, 0) mode increases, but that of the backward travelling wave of (3, 0) mode decreases, becoming unstable.

In case of $\varphi_s \neq 0$, Eqs. (28) and (29) can be rewritten, respectively, as

$$\begin{aligned}\sigma_m^b = &-\alpha - P_m k_d[(\omega_{md} - m\Omega)\cos m\varphi_s - \alpha \sin m\varphi_s] \\ &- j[\omega_{md} - m\Omega - \alpha P_m k_d \cos m\varphi_s \\ &- (\omega_{md} - m\Omega) P_m k_d \sin m\varphi_s]\end{aligned} \tag{32}$$

$$\begin{aligned}\sigma_m^f = &-\alpha - P_m k_d[(\omega_{md} + m\Omega)\cos m\varphi_s + \alpha \sin m\varphi_s] \\ &+ j[\omega_{md} + m\Omega - \alpha P_m k_d \cos m\varphi_s \\ &+ (\omega_{md} + m\Omega) P_m k_d \sin m\varphi_s]\end{aligned} \tag{33}$$

Here, the second terms in the above equations suggest that the modes corresponding to $m|\varphi_s| > \pi/2$ become unstable as k_d increases, as already discussed in(Ellis and Mote, 1979). In particular, the forward travelling waves become more easily

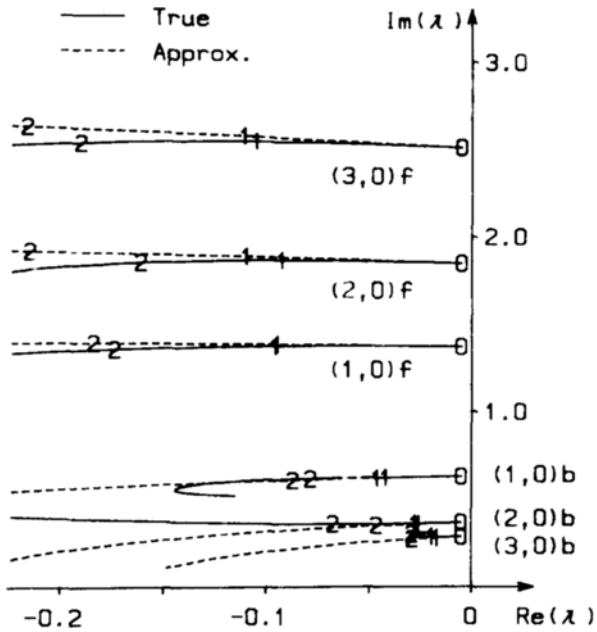

Fig. 7 Root loci of (1, 0), (2, 0) and (3, 0) modes as k_d increases when $\varphi_s = 10$ degrees (1 ; $k_d = 0.1$, 2 ; $k_d = 0.2$)

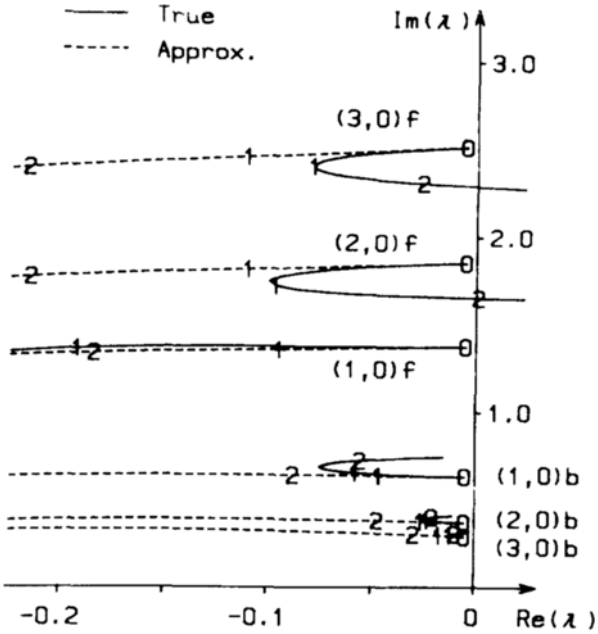

Fig. 8 Root loci of (1, 0), (2, 0) and (3, 0) modes as k_d increases when $\varphi_s = -10$ degrees (1 ; $k_d = 0.1$, 2 ; $k_d = 0.2$)

unstable. Figs. 7 and 8 show the loci of the closed-loop eigenvalues of the modes with 1 to 3 nodal diameters and zero nodal circle as the derivative gain k_d increases when the proportional gain k_p is zero and the sensor location is 10 and -10 degrees, respectively. As well as in Figs. (4) and (5), the solid lines are the loci of the closed-loop eigenvalues calculated from Eq. (19) when $N = 6$, and the dashed lines are the loci of the closed-loop eigenvalues obtained from the approximate solutions, Eqs. (30) and (31). As shown in Figs. 7 and 8, the true solutions have the same trends as the approximate solutions up to $k_d = 0.1$. In this range of k_d, the dampings of the forward travelling waves increase more rapidly than the backward travelling waves as expected in the analysis.

5. CONCLUSIONS

Output feedback control of rotating disk vibrations is investigated and the closed-loop system characteristics are analyzed in relation to the P-D gains and the sensor-actuator location, utilizing approximate solutions. Eigenvalue analyses in case of the half-clamped disk are also performed, with the gains and location varied. The conclusions can be made as follows :

(1) P-control tends to change the dampings of the forward and backward travelling waves in opposite ways. That is, for small positive φ_s, the dampings of the backward travelling waves of low frequencies, often considered important in the disk vibration, tend to increase as the proportional gain increases. However, for small negative φ_s, the dampings of the backward travelling waves of low frequencies tend to decrease as the proportional gain increases.

(2) D-control is likely to increase the dampings of the forward travelling waves more effectively than the backward travelling waves for small D-gain and small $|\varphi_s|$. This fact becomes more clear as the rotation speed increases. Therefore, D-control may result in an inefficient control performance when the backward travelling waves are of primary interest in the rotating disk vibration control problems.

REFERENCES

Byun, S.W., Lee, C.W., 1988 "Pole Assignment in Rotating Disk Vibration Control Using Complex Modal State Feedback," to appear in J. Mech. Sys. and Signal Processing, Vol. 2, No. 3 (in press)

Cho, H.S., Cho, Y.J., 1981, "Suboptimal Controller Design for Active Control of Circular Saw Vibrations," Optimal Control Applications and Methods, Vol. 2, pp. 299~310.

Ellis, R.W., Mote, C.D., Jr., 1979, "A Feedback Vibration Controller for Circular Saws," Trans. ASME, J. Dyn. Sys., Measurement and Control, Vol. 101, pp. 44~49.

Iwan, W.D., Moeller, T.L., 1976, "The Stability of a Spinning Elastic Disk with a Transverse Load System," Trans. ASME, J. Appl. Mech., Vol. 45, pp. 485~490.

Kato, T., 1966, "Perturbation Theory of Linear Operators," Springer Verlag, New York.

Kim, C.S., Lee, C.W., 1988 "Travelling Wave Control of Rotating Disks and Analysis of its Spillover Effect," to appear in Proc. Instn. Mechanical Engineers, Vol. 202, No. C2, pp. 119~127.

Mote, C.D., Jr., 1970, "Stability of Circular Plates Subjected to Moving Loads," J. Franklin Inst., Vol. 290, No. 4, pp. 329~344.

Mote, C.D., Jr., Holoyen, S., 1975, "Confirmation of the Critical Speed Theory for Symmetrical Circular Saws," Trans. ASME, J. Engineering for Industry, Vol. 97, No. 3, pp. 1112~1118.

Radcliffe, C.J., Mote, C.D., Jr., 1983, "Identification and Control of Rotating Disk Vibration, "Trans. ASME, J. Dyn. Sys., Measurement and Control, Vol. 105, pp. 39~45.